Bioorganic & Medicinal Chemistry Letters 20 (2010) 4095–4099

Contents lists available at ScienceDirect

Bioorganic & Medicinal Chemistry Letters

journal homepage: www.elsevier.com/locate/bmcl

Structure-based optimization of potent PDK1 inhibitors

Mauro Angiolini *, Patrizia Banfi, Elena Casale, Francesco Casuscelli, Claudio Fiorelli †, Maria B. Saccardo, Marco Silvagni, Fabio Zuccotto

Nerviano Medical Sciences Srl, Viale Pasteur 10, 20014 Nerviano, Milano, Italy

ARTICLE INFO

Article history:
Received 26 April 2010
Revised 17 May 2010
Accepted 18 May 2010
Available online 8 June 2010

Keywords:
Kinase
Structure-based drug design
PDK1
CDK2
Scaffold

ABSTRACT

In this Letter is described the structure-based design of potent dihydro-pyrazoloquinazolines as PDK1 inhibitors. Starting from low potency HTS hits with the aid of X-ray crystallography and modeling, a medicinal chemistry activity was carried out to improve potency versus PDK1 and selectivity versus CDK2 protein kinase.

Signal transduction of many growth factors and oncogenes is mediated by 3-phosphoinositide-dependent protein kinase-1 (PDK1), a master regulator of at least 23 related protein kinases belonging to the AGC kinase family.[1,2] PDK1 downstream transduction pathways involve a group of related serine-threonine protein kinases like AKT, p70 ribosomal S6 kinase, and PKC that mediate vital cell processes such as cell survival and proliferation. Moreover, about 50% of common human cancers including breast, lung, prostate, and blood possess overstimulation of the PDK1 signaling, making PDK1 an interesting therapeutic target in oncology.[3]

From the high throughput screening campaign of the corporate chemical collection carried out on PDK1, dihydro-pyrazoloquinazolines (general formula A—Fig. 1) emerged as one of the most interesting chemical classes based on good cell permeability data and a limited promiscuity profile compared to other active chemical classes identified. Unfortunately such a chemotype was also characterized by an intrinsic high affinity (nanomolar range) for CDK2 and PLK1 protein kinases.[4,5] In order to investigate the possibility of developing dihydro-pyrazoloquinazolines as PDK1 inhibitors, a medicinal chemistry project was started with the primary aim of improving potency against PDK1 and decreasing affinity versus CDK2.

Structural data related to both CDK2 and PDK1 kinases with the mode of binding of dihydro-pyrazoloquinazolines in CDK2 were available at project inception.[4b] In several years of research in the kinase field it has been observed that, with a few exceptions, the mode of binding of a particular scaffold is generally conserved amongst different kinases. We hence assumed that the mode of binding of scaffold A in PDK1 was similar to the one observed in CDK2. An analysis of the ATP binding pocket was performed in or-

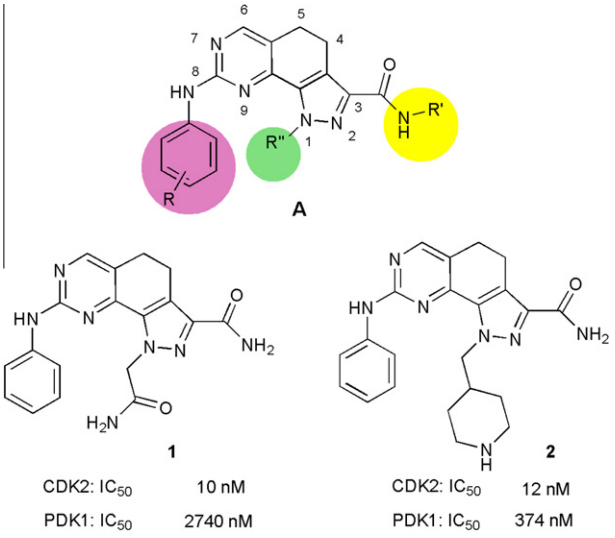

Figure 1. General structure of PDK1 dihydro-pyrazoloquinazolines inhibitors A and areas of potential SAR exploration. Chemical structures with biological activity of compounds **1**–**2**.

* Corresponding author. Tel.: +39 0331581518.
E-mail address: mauro.angiolini@nervianoms.com (M. Angiolini).
† Present address: Istituto Italiano di Tecnologia, via Morego 30, 16163 Genova, Italy.

0960-894X/$ - see front matter © 2010 Elsevier Ltd. All rights reserved.
doi:10.1016/j.bmcl.2010.05.070

Table 1
Different residues between CDK2 and PDK1 in the ATP binding region selected for increasing potency and selectivity

Location	CDK2	PDK1
Glycine loop	Glu8	Lys86
Glycine loop	Thr14	Ser92
Glycine loop	Tyr15	Phe93
Glycine loop	Gly16	Ser94
Gatekeeper	Phe80	Leu159
Hinge	Phe82	Tyr161
Hinge	Leu83	Ala162
Hinge	—	Asn164
Sugar region	Asp86	Glu166
Activation loop	Ala144	Thr222

der to identify differences that could be exploited for selective drug design. Interestingly the two binding sites are characterized by several different but structurally equivalent residues some of which could offer attractive opportunities in the development of PDK1 selective compounds (Table 1).

A chemical developability assessment of dihydro-pyrazoloquinazoline hits led to the selection of compound **1** (Fig. 1) as starting point for the optimization process despite its modest IC_{50} value against PDK1 and the potent activity in the low nanomolar range against CDK2.[6]

Dihydro-pyrazoloquinazoline **1** offered in fact several opportunities for SAR studies allowing access to different areas of the ATP binding site. With regard to the SAR exploration three regions of scaffold A were identified as crucial: the amide in position 3, the substitution on the nitrogen N1 of the pyrazole ring and the aromatic moiety installed on the amine in position 8 of the tricyclic scaffold (Fig. 1).

Based on our initial assumption of a CDK2-like binding mode for compound **1**, the primary amide on pyrazole N1 would be placed in proximity of Glu166 residue. The initial medicinal chemistry work hence focused on the optimization of the interaction between the ligand and the negatively charged side chain. As a result compound **2** (Fig. 1), prepared following a Mitsunobu protocol, was obtained displaying a sevenfold increase in potency versus PDK1 (IC_{50} = 374 nM) and an almost unvaried high potency versus CDK2 (12 nM).[5,7,8]

The 3D structure of the complex between PDK1 and compound **2** was solved by X-ray crystallography at 2.0 Å resolution confirming our initial assumption on the mode of binding of the dihydro-pyrazoloquinazoline scaffold in PDK1 (Fig. 2).[9–11] The scaffold indeed occupies the ATP pocket and binds to the hinge region

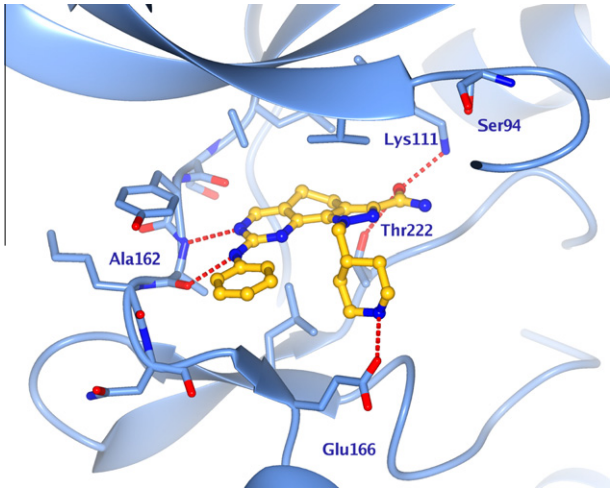

Figure 2. X-ray structure of compound **2** (PDB **2xch**) bound to PDK1 (blue ribbon) at 2.0 Å resolution. Hydrogen bonds are represented as red dashed lines.

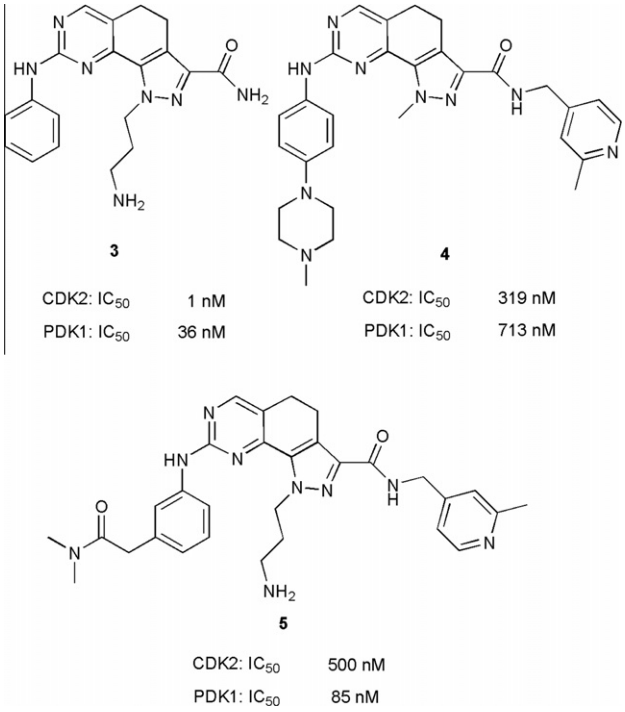

Figure 3. Chemical structure and biological activity for compounds **3**–**4**–**5**.

through the amino-pyrimidine moiety. A first hydrogen bond is established between the backbone NH of Ala162 and the nitrogen of the pyrimidine ring in position 7 and an additional hydrogen bond is observed between Ala162 carbonyl oxygen and the nitrogen of the anilino moiety in position 8 of the ligand. A further interaction between the conserved Lys111 and the carbonyl oxygen of the amide in position 3 of the pyrazole is also observed.

The structural data also confirmed that, as expected, the increased level of PDK1 related potency observed for compound **2** was the result of the favorable interaction between the positively charged nitrogen of the piperidine ring and the Glu166 side chain. The structurally equivalent residue in CDK2 is Asp86. Modeling work suggested that, despite its shorter side chain, Asp86 is capable of establishing the same type of interaction as confirmed by the good level of activity against CDK2 (12 nM). Clearly Glu166 could not be targeted for selectivity but it proved to be a key element to increase potency against PDK1. Further exploration of this interaction with linear chains containing basic residues like aminopropyl (compound **3**—Fig. 3) or aminoethyl (data not shown), allowed a significant and effective step towards low nanomolar PDK1 inhibitors but also led to even more potent CDK2 compounds. Compound **3** for instance had an IC_{50} value of 36nM against PDK1 and 1 nM against CDK2.

Having proved that dihydro-pyrazoloquinazolines could provide potent PDK1 inhibitors, the second phase of the chemistry project focused on targeting the CDK2 selectivity issue. In particular it was decided to follow two different strategies: one taking advantage of specific differences in aminoacids between the two kinases, the other one exploiting differences in the ATP binding site morphology. The work focused on two sub-regions: (1) a small cluster of residues (Ser92, Phe93, and Ser94) in the highly flexible glycine-rich loop that are different between PDK1 and CDK2 and (2) the hinge region, where the lack of a residue in CDK2 results in a different binding site shape and size in that area.

Knowing the ligand mode of binding, we hypothesized that secondary amide group in position 3 of the dihydro-pyrazoloquinazoline scaffold might be in direct contact with the terminal portion of the glycine-rich loop containing residues 92–94. An

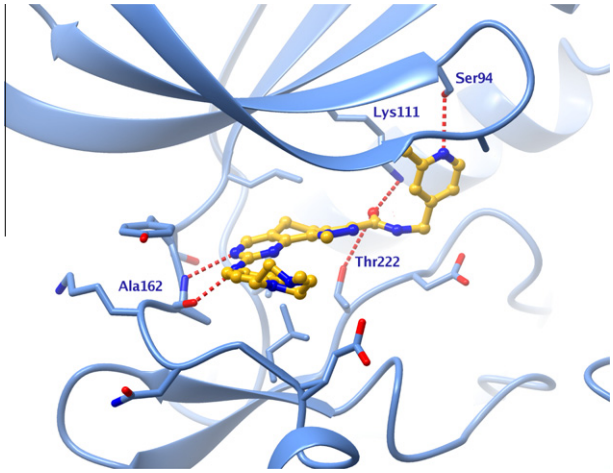

Figure 4. X-ray structure of compound **4** (PDB **2xck**) bound to PDK1 (2.3 Å resolution). Hydrogen bonds are represented as red dashed lines.

analysis of the HTS data related to the screened dihydro-pyrazoloquinazoline secondary amides, highlighted how substituents in this position could indeed modulate CDK2 activity. More important, bulky secondary amides showed a detrimental effect for CDK2 inhibition but still retaining activity versus PDK1. Compound **4**, for instance, one of the HTS hits belonging to this class, was characterized by an IC_{50} of 713 nM for PDK1 and an IC_{50} of 319 nM for CDK2. Moreover, docking studies of compound **4** in PDK1 suggested the pyridinyl moiety could engage Ser94 in the glycine-rich loop in an interaction with its sp^2 nitrogen.[12]

Structural studies of compound **4** bound to PDK1 confirmed the role of the 2-methyl-pyridin-4-ylmethyl amide in the kinase ATP binding site (Fig. 4).[11] As expected the pyridine ring sits underneath the glycine-rich loop with the 2-methyl group fitting nicely in a small cavity made up by Gly91 backbone and Ser94 and Thr95 side chains. Also, the pyridine sp^2 nitrogen establishes a hydrogen bond with Ser94 determining a further interaction for PDK1, as already observed by Feldman et al.[13]

Activity data obtained during the HTS for other members of the dihydro-pyrazoloquinazoline chemical class, suggested that typically an unsubstituted aniline in position 8 resulted in an enhanced

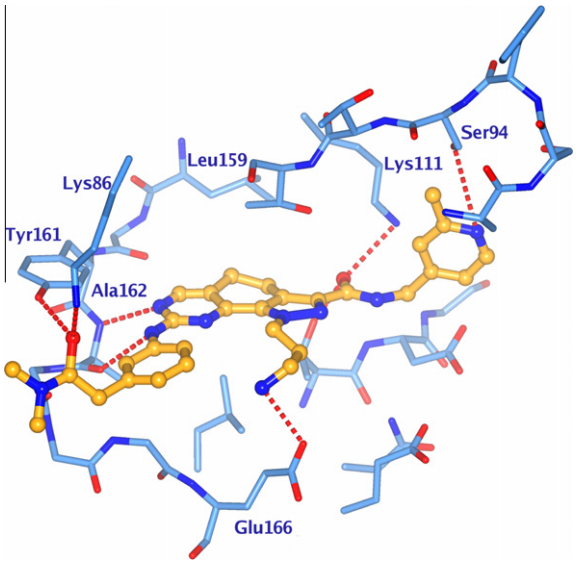

Figure 5. Docking model of compound **5** (yellow) bound to PDK1. Hydrogen bonds are represented as red dashed lines.

CDK2 activity. Similarly, *ortho*-substituted anilines were tolerated by CDK2 but resulted detrimental for PDK1 inhibition. Thus, in order to achieve potent PDK1 inhibitors having a selective profile versus CDK2 it was decided to design new derivatives containing both the amide moiety of compound **4** and the propylamino chain of compound **3** on pyrazole N1 and, at the same time, explore the *meta*-substitution on the aniline ring in position 8 to exploit the difference between the two kinases at the hinge region. In fact, in CDK2 the residue structurally equivalent to Asn164 in PDK1 is missing. The lack of this residue leads to a change in backbone conformation with the Leu83 and His84 carbonyl groups encroaching into the ATP binding site reducing the space available to the ligand. The idea we decided to follow was to introduce a group in this area so that it could be tolerated by PDK1 but less by CDK2 due to unfavorable steric clashes.

Modeling studies suggested that groups carrying hydrogen-bonding atoms could also offer the opportunity to establish additional and selective interactions with the PDK1 protein backbone. For instance, docking results suggested that the carbonyl group of the dimethyl amide in *meta*-position of compound **5** (Fig. 3) could give a hydrogen bond interaction with both positively charged Nε of Lys86 and the hydroxyl group of Tyr161, placing the dimethyl portion in the solvent exposed area at the same time (Fig. 5). The corresponding residues in CDK2 are, respectively, Glu8 and Phe82.[12]

Compound **5** was subsequently prepared and when tested showed an IC_{50} of 85 nM on PDK1. As expected the *meta*-substitution resulted in a further CDK2 activity loss with an IC_{50} of 500 nM, a significant 50-fold lower than the value obtained for structure **1**. The data confirmed that the secondary amide in position 3 is a key element to achieve the desired PDK1 selectivity profile versus CDK2. When tested in a kinases panel, compound **5** showed complete selectivity against Plk1, Gsk3-β, Lyn, Met, Mps1, Abl, Ack1, Akt1, Alk, Bub1, Kdr, Jak1, Jak3, Zap70, Cdc7, Irk, Jak2, Eef2k, Fak, p38α, Ret, Mst4, B-Raf, Ikk2, Igfr1, Egfr1, Fgfr1, Perk, Pak4, Brk, Ck2, Nek6, Lck, Sulu1, Nim, Mapkapk2, Syk, Tyk, TrkA. The kinases Aurora A (40 nM) and Aurora B (100 nM) were also inhibited by compound **5**.

The biological activity of the prepared compounds was also evaluated in a cell based assay using both A2780 ovarian and MCF7 breast cancer cell lines (Table 2).[14] The dihydro-pyrazoloquinazoline scaffold proved to have good cell permeability. Interestingly, compound **3** was one of the most active compounds on both cell lines despite the presence of the highly polar primary amine residue. Unfortunately, compound **5** displayed only residual activity in A2780 cell line. This is probably the result of different factors like a relatively low potency against PDK1, a detrimental effect of the specific substituents on the physicochemical properties of the molecule and a limited cross activity on other kinases (e.g., CDK2) which might be responsible for the cellular activity observed for compounds **2**, **3**, and **4**.

Scheme 1 reports the synthetic approach adopted to prepare the PDK1 inhibitor **5**.

Starting from the intermediate **6** the synthetic key step was the chemoselective introduction of the substituted anilino moiety at

Table 2
Cellular activities for compounds **1**–**5** in *A2780* and *MCF7* cell lines. Values are means of at least two experiments

Compound	A2780 (μM)	MCF7 (μM)
1	2.71	6.00
2	0.51	1.36
3	0.12	0.14
4	0.17	4.91
5	5.90	>10

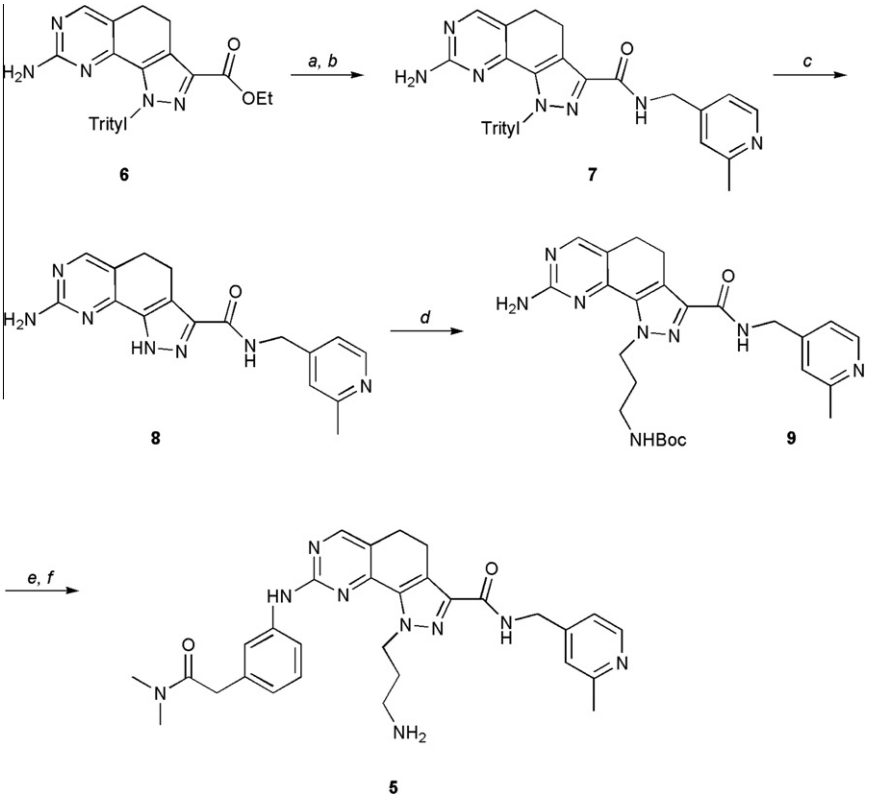

Scheme 1. Reagents and conditions: (a) KOH, EtOH, 50 °C, 90%; (b) DMF, 2-methyl-4-aminomethyl-pyridine, TBTU, DIPEA, 80%; (c) TFA, DCM, TES, rt, 75%; (d) Cs_2CO_3, DMF, *N*-Boc-propylamino-bromide, rt, 70%; (e) dioxane, 110 °C, 2% $Pd_2(dba)_3$, 4% Xantphos, 2-(3-iodo-phenyl)-*N*,*N*-dimethyl-acetamide, Cs_2CO_3, 60%; (f) HCl 4 M, dioxane, quantitative.

the position 8 of the tricyclic scaffold by the Hartwig–Buchwald reaction with dihydro-pyrazoloquinazoline derivative **9** as nucleophilic reagent.[6,15,16] This procedure avoided the low yield preparation of the 8-iodo-dihydro-pyrazoloquinazoline intermediate normally used for the arylation step.[4,5] Initial hydrolysis of the ethyl-ester **6** with potassium hydroxide and coupling with 2-methyl-4-aminomethyl-pyridine in presence of TBTU and DIPEA afforded intermediate **7** in 80% yield. Removal of trityl protective group from the pyrazole ring with trifluoroacetic acid furnished the compound **8** and alkylation with Cs_2CO_3 with the propyl-amino-bromide protected as Boc-derivative in DMF as solvent provided the compound **9** in good yield. The final product **5** was achieved by the Hartwig–Buchwald arylation carried out in dioxane with Xantphos as ligand reagent, aryl-iodide and $Pd_2(dba)_3$ as the most efficient catalyst in 60% yield. Treatment with HCl 4 M in dioxane afforded the final compound **5**.[17]

In summary, HTS dihydro-pyrazoloquinazolines hits were optimized to increase PDK1 potency and to falter activity on CDK2. Potency was increased about 75-fold (compound **1**—PDK1 IC_{50} = 2740 nM, compound **3**—PDK1 IC_{50} = 36 nM) establishing charge interactions with Glu166 whereas selectivity towards CDK2 was obtained by developing secondary amide analogues (PDK1/CDK2 activity ratio was improved from 274 for compound **1** to 0.17 for compound **5**). The strategy was supported by crystallographic confirmation of the mode of binding of the analyzed compounds. Further optimization is required to achieve a therapeutic level of cellular activity.

Acknowledgments

We would like to thank Daniele Donati and Gabriella Brasca for valuable discussions; Francesca Quartieri and Roberto Marcucci for supporting the chemistry activity.

References and notes

1. Pearce, L. R.; Komander, D.; Alessi, D. R. *Nat. Rev. Mol. Cell. Biol.* **2010**, *11*, 9.
2. Mora, A.; Komander, D.; van Aalten, D. M. F.; Alessi, D. R. *Semin. Cell Dev. Biol.* **2004**, *15*, 161.
3. (a) Atkinson, F. L.; Axten, J. M.; Cichy-Knight, M.; Moore, M. L.; Patei, V. K.; Tian, X.; Wellaway, C. R.; Dunn, A. K. WO2010/019637, 2010.; (b) Nittoli, T.; Dushin, R. G.; Ingalls, C.; Cheung, K.; Floyd, M. B.; Fraser, H.; Olland, A.; Hu, Y.; Grosu, G.; Han, X.; Arndt, K.; Guo, B.; Wissner, A. *Eur. J. Med. Chem.* **2010**, *45*, 1379; (c) Wuchrer, M.; Bruge, D.; Finsinger, D.; Graedler, U.; Dorsch, D.; Esdar, C. WO2010/000364, 2010.; (d) Ramurthy, S.; Jain, R.; Lin, X.; NG, S. C.; Pfister, K. B.; Rico, A.; Subramanian, S.; Wang, X. M. WO2009/153313, 2009.; (e) Kim, K. H.; Wissner, A.; Floyd, M. B., Jr.; Fraser, H. L.; Wang, Y. D.; Dushin, R. G.; Hu, Y.; Olland, A.; Guo, B.; Arndt, K. *Bioorg. Med. Chem. Lett.* **2009**, *19*, 5225; (f) Iorns, E.; Lord, J. C.; Ashworth, A. *Biochem. J.* **2009**, *417*, 361; (g) Maira, S.-M.; Furet, P.; Stauffer, F. *Fut. Med. Chem.* **2009**, *1*, 137; (h) Stauffer, F.; Maira, S. M.; Furet, P.; Garcìa-Echeverrìa, C. *Bioorg. Med. Chem. Lett.* **2008**, *18*, 1027; (i) Peifer, C.; Alessi, D. R. *ChemMedChem* **2008**, *3*, 1810.
4. 4a Traquandi, G.; Ciomei, M.; Ballinari, D.; Casale, E.; Colombo, N.; Croci, V.; Fiorentini, F.; Isacchi, A.; Longo, A.; Mercurio, C.; Panzeri, A.; Pastori, W.; Pevarello, P.; Volpi, D.; Roussel, P.; Vulpetti, A.; Brasca, M. G. *J. Med. Chem.* **2010**, *53*, 2171; (b) Brasca, M. G.; Traquandi, G.; Vianello, P.; Quartieri, F.; Panzeri, A.; Pevarello, P.; Vulpetti, A.; Roletto, F.; D'Alessio, R.; Amboldi, N.; Ballinari, D.; Cameron, A.; Casale, E.; Cervi, G.; Colombo, M.; Colotta, F.; Croci, V.; Fiorentini, F.; Isacchi, A.; Mercurio, C.; Moretti, W.; Pastori, W.; Ciomei, M. *J. Med. Chem.* **2009**, *52*, 5152.
5. Beria, I.; Brasca, M. G.; Caruso, M.; Ballinari, D.; Borghi, D.; Bossi, R. T.; Cappella, P.; Ceccarelli, W.; Ciavolella, A.; Cristiani, C.; Croci, V.; De Ponti, A.; Fachin, G.; Ferguson, R. D.; Lansen, J.; Moll, J.; Pesenti, E.; Posteri, H.; Perego, P.; Rocchetti, M.; Volpi, D.; Valsasina, B.; Bertrand, J. A.; Storici, P. *J. Med. Chem.* **2010**, *53*, 3532.
6. Traquandi, G.; Brasca, M. G.; Polucci, P.; Vianello, P.; Ferguson, R.; Quartieri, F.; Panzeri, A.; Pevarello, P.; Vulpetti, A.; Roletto, F.; D'Alessio, R.; Fancelli, D. WO2004/104007, 2004.
7. Caruso, M.; Beria, I.; Brasca, M. G.; Ferguson, R. D.; Posteri, H.; Valsasina, B. WO2008/074788, 2008.
8. *In vitro kinase activity assays*: IC_{50} values were determined as reported in Ref. 6.
9. Biondi, R. M.; Komander, D.; Thomas, C. C.; Lizcano, J. M.; Deak, M.; Alessi, D. R.; van Aalten, D. M. *EMBO J.* **2002**, *21*, 4219.
10. (a) Otwinowski, Z.; Minor, W.. In *Methods in Enzymology*; Carter, C. W., Sweet, R. M., Eds.; Academic Press: San Diego, 1997; Vol. 276, pp 307–326; (b) Emsley, P.; Cowtan, K. *Acta Crystallogr., Sect. D* **2004**, 2126.

11. Crystals for soaking were transferred to a solution of 2.2 M ammonium sulfate, 0.1 Tris pH 8.5, 20% glycerol in which compounds **2** and **4** were dissolved up to saturation. Diffraction data were collected at the ESRF (Grenoble, France). Data were processed using the HKL package (Otwinoski and Minor, 1997). Model correction and structure refinement were iteratively carried out with COOT (Emsley, 2004) and Refmac (CCP4, 1994). The final R-factor achieved for each complex was of 20.2% (Rfree 23.3%) for compound **2** and 20.5% (Rfree 24.4%) for compound **4**. Crystallographic data with the corresponding structure factors files for compounds **2** and **4** have been deposited with the Protein Data Bank (PDB) under the accession code **2xch** and **2xck**.
12. Docking simulations were carried out using the mcdock algorithm implemented in the FLO_QXP package: McMartin, C.; Bohacek, R. S. *J. Comput. Aided Mol. Des.* **1997**, *11*, 333.
13. Feldman, R. I.; Wu, J. M.; Polokoff, M. A.; Kochanny, M. J.; Dinter, H.; Zhu, D.; Biroc, S. L.; Alicke, B.; Bryant, J.; Yuan, S.; Buckman, B. O.; Lentz, D.; Ferrer, M.; Withlow, M.; Adler, M.; Finster, S.; Chang, Z.; Arnaiz, O. D. *J. Biol. Chem.* **2005**, *280*, 19867.
14. *Cellular assays*: *A2780* (ECACC) were grown in an RPMI-1640 medium supplemented with heat-inactivated 10% fetal calf serum. *MCF7* (ECACC) were grown in MEM medium supplemented with heat-inactivated 10% fetal calf serum. Cells were seeded at different densities ranging from 2500 to 5000 cells/well in black 96-well plates with the appropriate complete medium. After 24 h the plates were treated with the compound to be tested and incubated for 72 h at 37 °C under a 5% CO_2 atmosphere. At the end of the incubation, cells were lysed and the ATP content in the well used as a measure of viable cells. This was determined with a thermostable firefly luciferase based assay (CellTiter-Glo) from Promega. IC_{50} values were calculated with the rate of percent of growth versus the untreated control.
15. Yin, J.; Zhao, M. M.; Huffman, M. A.; McNamara, J. M. *Org. Lett.* **2002**, *20*, 3481.
16. Loones, K. T. J.; Maes, B. U. W.; Dommisse, M. A.; Lemière, G. L. F. *Chem. Commun.* **2004**, *21*, 2466.
17. Procedure for the synthesis of compound **5** by the Hartwig–Buchwald reaction (Step (e) of Scheme 1). To a suspension of (3-{8-amino-3-[2-methyl-pyridin-4-ylmethyl)-carbamoyl]-4,5-dihydro-1,2,7,9-tetraaza-cyclopenta[*a*]naphthalen-1-yl}-propyl)-carbamic acid-*tert*-butyl ester (0.142 mmol; 1 equiv) **9** in dry dioxane (1.5 ml) under argon atmosphere, Cs_2CO_3 (0.2 mmol; 1.4 equiv), Xantphos (0.0056 mmol; 0.04 equiv), $Pd_2(dba)_3$ (0.0028 mmol; 0.02 equiv) and 2-(3-iodo-phenyl)-*N*,*N*-dimethyl-acetamide (0.2 mmol; 1.4 equiv) were added. The suspension was heated 8 h at 100 °C and the solvent removed in vacuum. The residue extracted in DCM-water was purified by flash column chromatography (AcOEt/MeOH 98:2) affording the corresponding product as Boc-protected compound in 60% yield. Final treatment with 10 equiv of HCl 4 M in dioxane gave compound **5** as a white hydrochloride salt. ^{1}H NMR (400 MHz, DMSO): δ 2.15 (q, 2H, $NCH_2CH_2CH_2NH_2$, J = 6.58 Hz), 2.73 (s, 3H, CH_3Pyr), 2.80–2.85 (m, 4H, $NCH_2CH_2CH_2NH_2$, $-CH_2CH_2-$), 2.86 (s, 3H, CH_3NCH_3CO), 3.00 (t, 2H, $-CH_2CH_2-$, J = 7.56 Hz), 3.03 (s, 3H, CH_3NCH_3CO), 3.69 (s, 2H, $ArCH_2CONMe_2$), 4.65 (d, 2H, $CONHCH_2Pyr$, J = 5.97 Hz), 4.90 (t, 2H, $NCH_2CH_2CH_2NH_2$, J = 6.58 Hz), 6.86 (d, 1H, HAr, J = 7.68 Hz), 7.27 (t, 1H, HAr, J = 7.68 Hz), 7.50 (br s, 1H, HAr), 7.62 (d, 1H, HAr, J = 7.68 Hz), 7.77 (d, 1H, HPyr, J = 6.34 Hz), 7.82 (br s, 1H, HPyr), 7.97 (br s, 3H, $NCH_2CH_2CH_2NH_2{\cdot}HCl$), 8.43 (s, 1H, HPyrim), 8.71 (d, 1H, HPyr, J = 6.34 Hz), 9.10 (t, 1H, $CONHCH_2Pyr$, J = 5.97 Hz), 9.59 (s, 1H, NHPyrim). HRMS calcd for $C_{30}H_{36}N_9O_2$ (MH^+): 554.2987. Found: 554.2982.